View metadata, citation and similar papers at core.ac.uk
brought to you by CORE
provided by Institutional Repository of Institute of Earth Environment, CAS

Aerosol and Air Quality Research, 18: 397–406, 2018
Copyright © Taiwan Association for Aerosol Research
ISSN: 1680-8584 print / 2071-1409 online
doi: 10.4209/aaqr.2017.02.0070

Seasonal Characteristics of Black Carbon Aerosol and its Potential Source Regions in Baoji, China

Bianhong Zhou[1,2], Qiyuan Wang[2*], Qi Zhou[1], Zhangquan Zhang[1], Gehui Wang[2], Ni Fang[1], Meijuan Li[1], Junji Cao[2,3]

[1] *Department of Geography and Environmental Engineering, Shaanxi Key Laboratory of Disaster Monitoring and Mechanism Simulation, Baoji University of Arts and Sciences, Baoji 721013, China*
[2] *Key Laboratory of Aerosol Chemistry and Physics, State Key Laboratory of Loess and Quaternary Geology, Institute of Earth Environment, Chinese Academy of Sciences, Xi'an 710061, China*
[3] *Institute of Global Environmental Change, Xi'an Jiaotong University, Xi'an 710049, China*

ABSTRACT

Continuous measurements of black carbon (BC) aerosol were made at a midsized urban site in Baoji, China, in 2015. The daily average mass concentrations varied from 0.6 to 11.5 μg m^{-3}, with an annual mean value of 2.9 ± 1.7 μg m^{-3}. The monthly variation indicated that the largest loading of BC occurred in January and the smallest in June. The mass concentrations exhibited strong seasonality, with the highest occurring in winter and the lowest in summer. The large BC loadings in winter were attributed to the increased use of fuel for domestic heating and to stagnant meteorological conditions, whereas the low levels in summer were related to the increase in precipitation. BC values exhibited similar bimodal diurnal patterns during the four seasons, with peaks occurring in the morning and evening rush hours and an afternoon trough, which was associated with local anthropogenic activities and meteorological conditions. A potential source contribution function model indicated that the effects of regional transport mostly occurred in spring and winter. The most likely regional sources of BC in Baoji were southern Shaanxi province, northwestern Hubei province, and northern Chongqing during spring, whereas the northeastern Sichuan Basin was the most important source region during winter.

Keywords: Black carbon aerosol; Seasonal characterization; Diurnal variation; Potential source region.

INTRODUCTION

Atmospheric aerosols are a widespread concern due to their physicochemical role in atmospheric processes, which can cause them to disturb the solar radiative balance of the earth (Bellouin *et al.*, 2005; Gordon *et al.*, 2016). The uncertainty regarding the radiative forcing induced by atmospheric particulate matter is a major obstacle to the accurate prediction of climate change (Kahn, 2012; Lee *et al.*, 2016). Black carbon (BC) aerosol, which is a byproduct of the incomplete combustion of carbon-containing fuels, can strongly absorb radiation over a wide wavelength range, ranking as the second largest contributor to positive radiative forcing in the atmosphere after CO_2 (Bond *et al.*, 2013) The estimated direct radiative forcing of BC ranges from 0.2 to 0.8 W m^{-1} (Jacobson, 2001; Kim *et al.*, 2008; Bond *et al.*, 2011), representing a sizeable contribution to atmospheric heating even at the lower end value. BC is chemically inert and is mainly concentrated in the accumulation mode with diameters of 0.01–1.0 μm (Bond *et al.*, 2013). These physicochemical characteristics cause BC to have an atmospheric lifetime of approximately one week, making it amenable to long-range transport to other regions (Liu *et al.*, 2011; Wang *et al.*, 2015; Targino and Krecl, 2016). Moreover, BC is an important component of air pollution in urban areas, exacerbating the degradation of visibility (Zhou *et al.*, 2012; Wang *et al.*, 2013). In addition, direct inhalation of BC particles has been found to cause vascular, cardiopulmonary, and respiratory diseases (Janssen *et al.*, 2011; Heal *et al.*, 2012).

China has been recognized as the most important emitter of BC in East Asia (Xiao *et al.*, 2014). In 2008, the total BC emission in China was estimated to be 1604.94 Gg, with 695.03 Gg, 636.02 Gg, and 194.63 Gg contributed by industry, the residential sector, and transportation, respectively. These three sources together contributed approximately 95% of the total BC (Zhang *et al.*, 2013a). During the past decade, a number of measurements have been carried out in urban areas of China—for instance, in the Beijing–Tianjin–Hebei region (Chen *et al.*, 2016; Wang *et al.*, 2016a), Yangtze River Delta area (Feng *et al.*, 2014;

*Corresponding author.
E-mail address: wangqy@ieecas.cn

Zhuang *et al.*, 2014; Shen *et al.*, 2015), Pearl River Delta area (Wu *et al.*, 2013; Chen *et al.*, 2014; Gong *et al.*, 2015), and Guanzhong Basin (Zhuang *et al.*, 2014; Wang *et al.*, 2016b). Many valuable data on the characterization of BC mass concentration have been obtained in China. However, most of the studies involved short-term measurements and mainly focused on the provincial capital or highly developed cities. By contrast, few studies have addressed midsized cities. The different energy structure and types of energy consumption between large and mid-sized cities can lead to differences in BC emission. For example, more BC from biomass burning were found in midsized cities than large cities (Wang *et al.*, 2012).

Knowledge of seasonal variations in BC is important as it enables the effect of BC emissions on regional climate to be assessed. The measurement site in our study, Baoji (106.30–108.05°E, 33.58–35.10°N), is the second largest city of Shaanxi province located on the west of the Guanzhong Plain at the southern edge of the Loess Plateau. It has a resident population of > 0.75 million. Rapid urbanization has led to the visibility in Baoji exhibiting a decreasing trend since 1997, indicating a progressive degradation of air quality (Xiao *et al.*, 2014). In excess of approximately 40% of the Chinese cities have a similar population and level of economic development to Baoji (Wu, 2004); the seasonal characteristics of BC analysis identified in this study may have important reference value for air pollution control in midsized cities in China. Therefore, the primary objectives of this study were (1) to investigate the seasonal and diurnal variations of BC and (2) to evaluate the potential sources for BC.

EXPERIMENTAL METHODS

The seasonal characteristics of BC aerosol were studied in samples collected at an inland urban site in Baoji (Fig. 1). Measurements of BC were conducted on the rooftop of a six-floor building at the Baoji University of Arts and Sciences (107.20°E, 34.35°N, approximately 18 m above ground level) from January 1 to December 31 2015. The sampling site is surrounded by educational and residential districts. To the north is a moderately busy two-lane road (approximately 30 m) while to the west is another moderately traveled two-lane road. There are no major industrial sources located nearby. This sampling site is representative of the urban conditions of Baoji.

The 5-minute averaged BC mass concentration was measured with an aethalometer (Model AE-31, Magee Scientific, Berkley, CA, USA) using the optical attenuation technique. Ambient air was drawn into the aethalometer at a flow rate of 5 L min^{-1} with a 2.5 μm cut-point inlet cyclone. Descriptions of the instrument and operational principle have been provided elsewhere (Virkkula *et al.*, 2007; Cheng *et al.*, 2010; Wu *et al.*, 2012). Briefly, the AE-31 model can

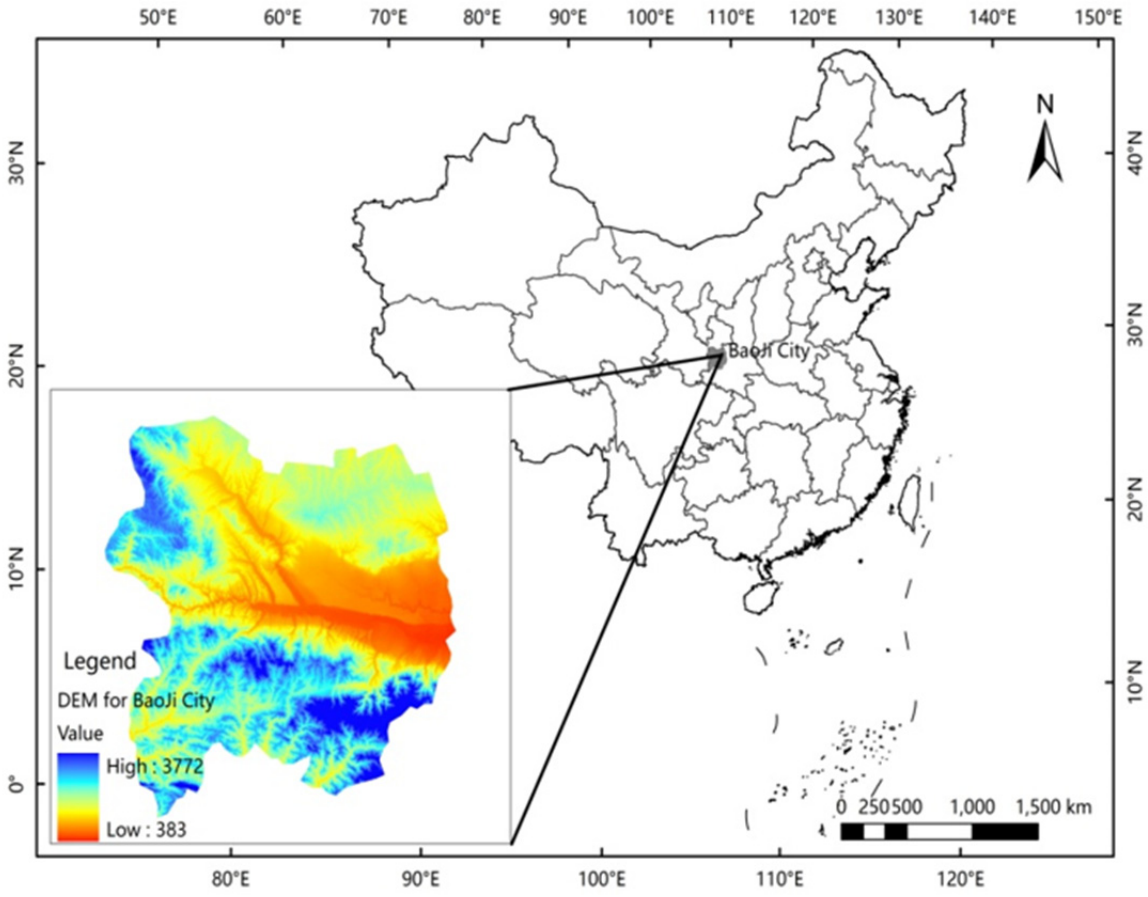

Fig. 1. Location of the Baoji sampling site.

measure optical attenuation at seven wavelengths (370, 470, 520, 590, 660, 880, and 970 nm). After ambient particles are collected on the filter, the aethalometer measures the attenuation of the light beam at each target wavelength transmitted through the filter. The instrument has two photodetectors: one is a reference beam that measures the light intensity passing through the pristine portion of the filter, and the other is a sensing beam that measures the same light crossing the particle-laden filter. The attenuation at each wavelength is then estimated from the intensity difference of the sensing and reference beams. The manufacturer of the aethalometer states an error of < 5% in the measurement of BC mass concentration. Based on the error budget discussed in several previous studies, the maximum uncertainty in the measured BC mass concentration is 20%, with a larger percentage of error being applicable to very low BC loadings (Corrigan *et al.*, 2006; Moorthy *et al.*, 2007; Nair *et al.*, 2007). Previous studies indicate that the filter-based measurements by attenuation method can be suffered from light scattering artifacts (Arnott *et al.*, 2005; Virkkula *et al.*, 2007; Rattigan *et al.*, 2013). Thus, a simple method for correcting the loading effects of aethalometer raw data was used in this study, which was based on the formula of $BC_{corrected} = (1 + k \times ATN) \times BC_{noncorrected}$, where ATN is the light attenuation and BC is the black carbon. The k used here was 0.0007 for summer and 0.0054 for the other seasons following Virkkula *et al.* (2007).

Hourly averaged meteorological data, including temperature, wind speed, and precipitation, were obtained from the Baoji Meteorological Bureau, which is approximately 7 km from the sampling site. Daily averaged concentration of sulfur dioxide (SO_2) was measured at Baoji Environmental Monitoring Station.

RESULTS AND DISCUSSION

Monthly and Seasonal Variations of BC Mass Concentration

The daily average mass concentration of BC from January 1 to December 31, 2015, is shown in Fig. 2. Daily average BC mass concentrations ranged by > 19-fold from 0.6 to 11.5 μg m^{-3}, with considerable day-to-day variation. The annual arithmetic mean (± standard deviation) concentration of BC was 2.9 ± 1.7 μg m^{-3}.The data in Table 1 indicate that the annual average BC mass concentration in Baoji was lower relative to those of some urban areas of China such as Beijing (6.3 μg m^{-3} (Zhao *et al.*, 2013)), Guangzhou (4.7 μg m^{-3} (Chen *et al.*, 2014)), Chengdu (10.8 μg m^{-3} (Zhang *et al.*, 2012)), Xi'an (14.7 μg m^{-3} (Cao *et al.*, 2009)), Nanjing (4.2 μg m^{-3} (Zhuang *et al.*, 2014)), and Xianghe (4.9 μg m^{-3} (Ran *et al.*, 2016)), and that it was comparable to those of Shanghai (3.3 μg m^{-3} (Feng *et al.*, 2014)) and Hefei (3.5 μg m^{-3} (Zhang *et al.*, 2015)). Compared with areas outside China, the annual mean BC mass concentration in Baoji was similar to or higher than the levels reported for Toulon, France (0.6 μg m^{-3} (Saha and Despiau, 2009)), Granada, Spain (3.0 μg m^{-3} (Lyamani *et al.*, 2011)), Anantapur, India (3.0 μg m^{-3} (Reddy *et al.*, 2012)), and Mexico City (0.9–3.1 μg m^{-3} (Retama *et al.*, 2015)), but lower than those of Delhi, India (6.7 μg m^{-3}, (Tiwari *et al.*, 2013)) and Kathmandu, Nepal (11.6 μg m^{-3}, (Putero *et al.*, 2015)). The differences in the BC mass concentrations can be attributed to the distinct emission sources and meteorological conditions as well as the different methods and times of year applied for BC measurement.

The variation of monthly averaged BC concentrations (Fig. 3) indicates that the BC mass concentration started to increase from June and peaked throughout the winter period. The highest monthly BC mass concentration was found in January and was higher than the lowest value in June by a factor of 3.6. In January, the mean wind speed was 1.2 m s^{-1}, with conditions typically being calm. Although the mean wind speed varied within a narrow range of 0.9–1.5 m s^{-1} from month to month during the entire campaign, temperatures were lowest in January and had an average value of 2.3°C. The residents of the town and surrounding areas usually burn coal or biomass (e.g., straw and/or wood) for domestic heating during winter. Burning these fuels in domestic conditions typically results in the emission of large BC particles. Because January is the coldest month,

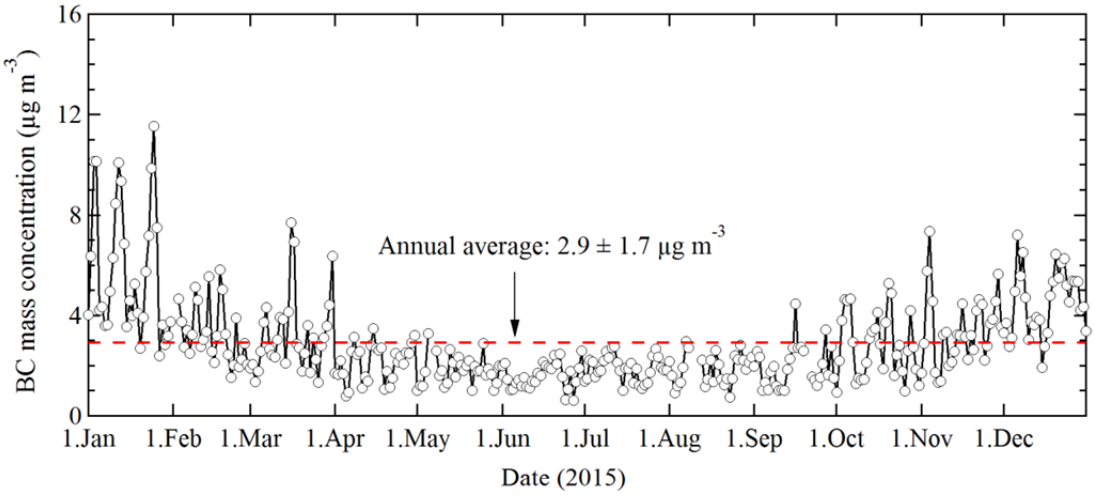

Fig. 2. Daily variation of the measured BC mass concentration during the entire campaign.

Table 1. Average black carbon (BC) mass concentrations at selected locations.

Location	Observation period	BC (μg m^{-3})	Reference
Baoji	Jan.–Dec. 2015	2.9 ± 1.7	This study
Beijing	2009–2010	6.3 ± 2.9	Zhao *et al.*, 2013
Guangzhou	Dec. 2007–Dec. 2008	4.7	Chen *et al.*, 2014
Chengdu	2006–2007	10.8 ± 5.5	Zhang *et al.*, 2012
Xi'an	Sep. 2003–Aug. 2005	14.7 ± 9.5	Cao *et al.*, 2009
Nanjing	Jan. –Dec. 2012	4.2 ± 2.6	Zhuang *et al.*, 2014
Xianghe	Apr. 2014–Mar. 2015	4.9 ± 4.3	Ran *et al.*, 2016
Shanghai	Jan.–Dec. 2011	3.3 ± 2.1	Feng *et al.*, 2014
Hefei	Jun. 2012–May 2013	3.5 ± 2.5	Zhang *et al.*, 2015
Toulon, France	Oct. 2005–Oct. 2006	0.6 ± 0.4	Saha and Despiau, 2009
Delhi, India	Jan.–Dec. 2011	6.7 ± 5.7	Tiwari *et al.*, 2013
Anantapur, India	Jan.–Dec. 2010	3.0 ± 0.3	Reddy *et al.*, 2012
Mexico City	Mar. 2013–Mar. 2014	0.9-3.1	Retama *et al.*, 2015
Kathmandu, Nepal	Feb. 2013–Jan.2014	11.6 ± 10.7	Putero *et al.*, 2015
Granada, Spain	Dec. 2005–Nov. 2008	3.0 ± 1.5	Lyamani *et al.*, 2011

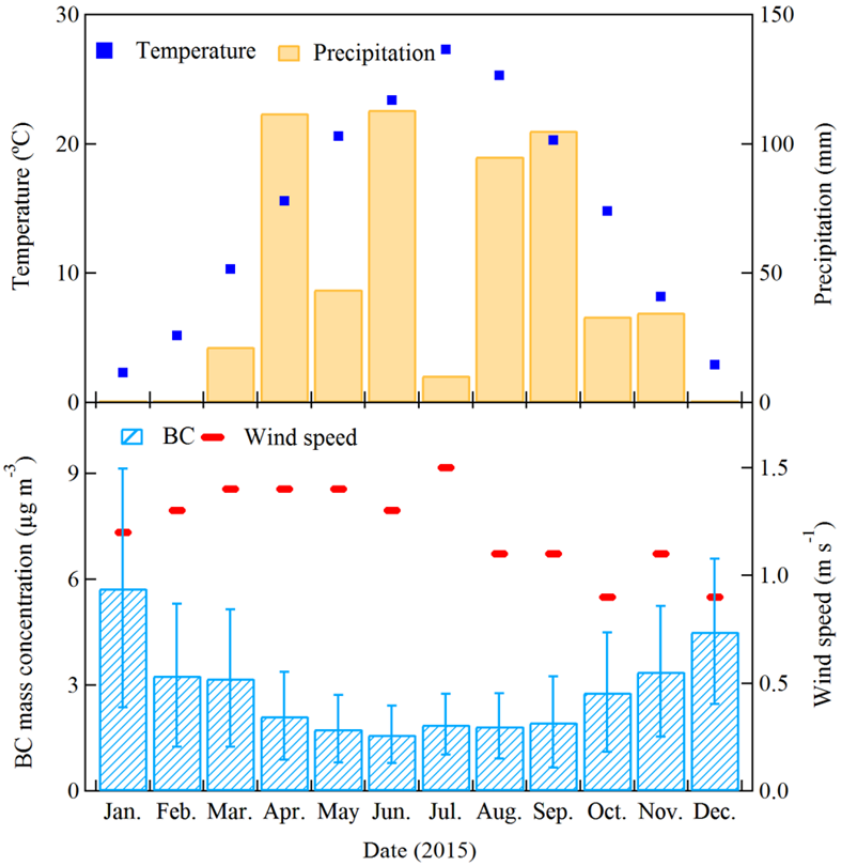

Fig. 3. Seasonal average BC mass concentrations, wind speed, temperature, and precipitation.

more fuel is burned than during other winter months. This resulted in the highest BC loadings. In comparison, in June, approximately 35% of sampling days had rainfall, which was the highest of all months. Precipitation is the most effective means of removing BC from the atmosphere, resulting in the lowest values of BC occurring in June.

Frequency distributions of BC mass concentrations for each season are shown in Fig. 4, with the total 5-minute averaged data divided into a finer mass interval of 1 μg m^{-3}. As illustrated in this figure, the mass concentrations of BC followed a typical lognormal pattern in all seasons. The BC mass concentrations showed obvious seasonal variations with the highest value of 4.6 ± 2.8 μg m^{-3} in winter (December–February) and lowest value of 1.8 ± 0.9 μg m^{-3} in summer (June–August). The seasonal average BC mass concentrations in spring and autumn were comparable, with the values being 2.4 ± 1.6 and 2.7 ± 1.7 μg m^{-3}, respectively. Most BC values concentrated within the range of 1–5 μg m^{-3} (Fig. 4),

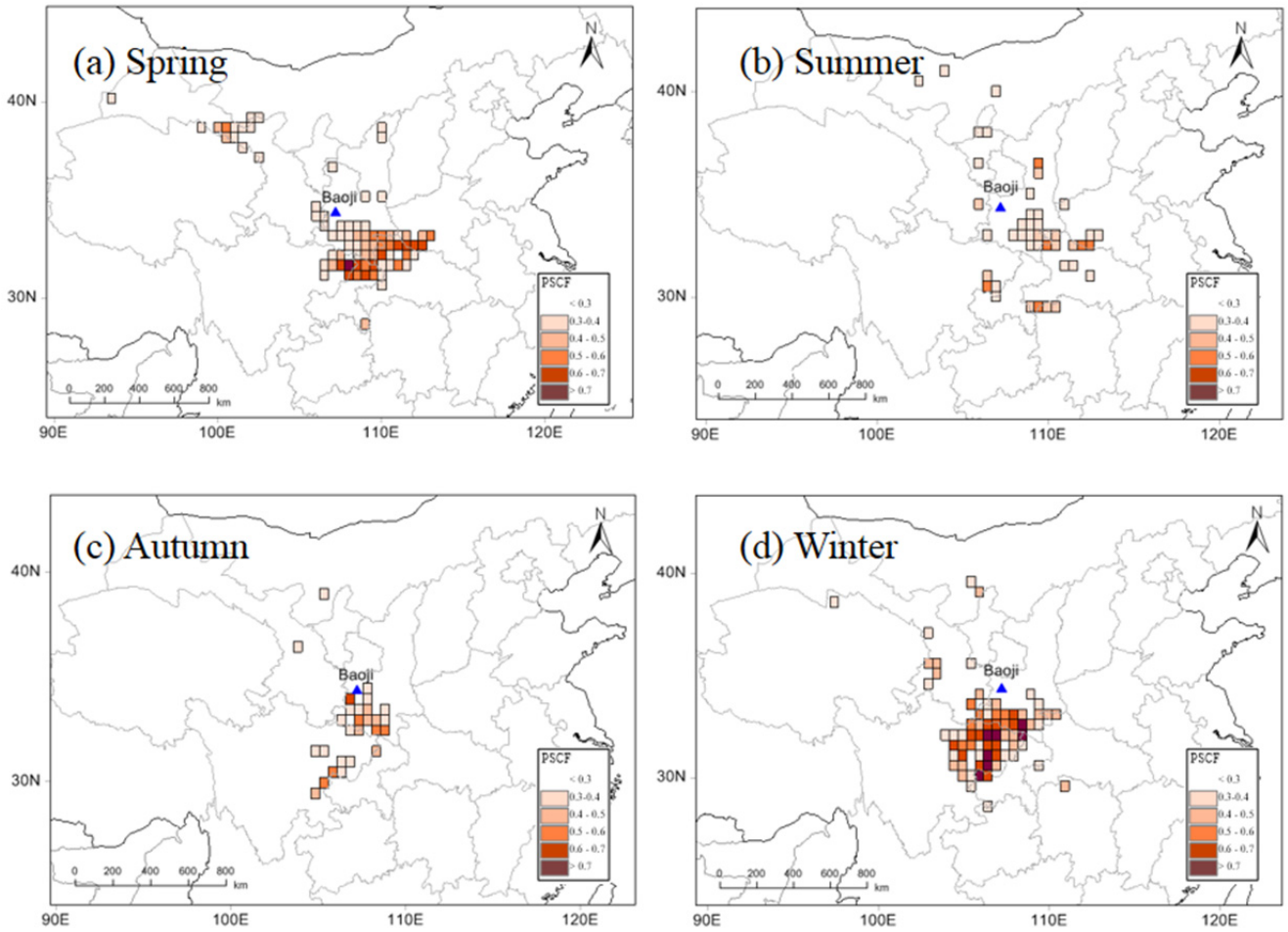

Fig. 4. Frequency distributions of hourly average BC concentrations during the four seasons. The vertical red dash lines represent the seasonal average mean values.

accounting for approximately 77%, 78%, 77%, and 61% of the total data samples from spring to winter, respectively. The maximum frequencies of 30%, 42%, 28%, and 17% occurred at the ranges from 1.0 to 2.0 μg m^{-3}, 1.0 to 2.0 μg m^{-3}, 2.0 to 3.0 μg m^{-3}, and 3.0 to 4.0 μg m^{-3} in spring, summer, autumn, and winter, respectively. From spring to autumn, the frequency of high BC values was mostly observed in smaller bin regions, while in winter, they occurred in larger bin regions. The frequency of BC values > 10 μg m^{-3} was substantially high in winter, possibly due to the increased domestic heating activities and stagnant meteorological conditions. BC values ranging from 8 to 10 μg m^{-3} can also appear in spring and autumn, during which BC levels can be dramatically enhanced by pollution episodes.

The seasonality of BC was attributed to the seasonal variations of anthropogenic emission sources as well as meteorological conditions (e.g., wind speed and rainfall). The large BC loadings in winter were related to domestic heating activities using coal combustion to warm the house. This can be further proved by the higher SO_2 concentration in winter (27.4 μg m^{-3}) than in other seasons (12.9, 5.3, and 9.5 μg m^{-3} for spring, summer, and autumn, respectively). Moreover, the more frequent occurrences of stagnant meteorological conditions (e.g., low atmospheric boundary layer and wind speed) can aggravate the BC accumulation on the surface. The low BC levels in summer were possibly due to high convective activity, which can cause BC dilution. Furthermore, the enhanced precipitation is another important factor leading to low BC in summer. The seasonal variations of BC at Baoji are consistent with those observed in other urban areas of China (e.g., Cao *et al.*, 2009; Zhuang *et al.*, 2014; Zhang *et al.*, 2015) in which higher BC mass concentrations occurred in winter.

Diurnal Variations of BC Mass Concentration

Diurnal variations of BC can effectively reflect the role of local anthropogenic activities and mesoscale atmospheric processes (Reddy *et al.*, 2012). Fig. 5 illustrates the diurnal variations of BC during four seasons in Baoji. The BC mass concentrations exhibited similar bimodal diurnal patterns in each season. The BC values started to increase in the morning at 04:00–05:00, with the highest increasing rate being 0.8 μg m^{-3} h^{-1} in winter and 0.3–0.4 μg m^{-3} h^{-1} in the other seasons; it then attained a morning peak at 07:00–08:00, with a value of 3.2 μg m^{-3} for spring, 2.5 μg m^{-3} for summer, 2.9 μg m^{-3} for autumn, and 6.3 μg m^{-3} for winter. Thereafter, BC decreased at a certain rate of 0.3, 0.2, 0.2, and 0.8 μg m^{-3} h^{-1} from spring to winter, respectively and

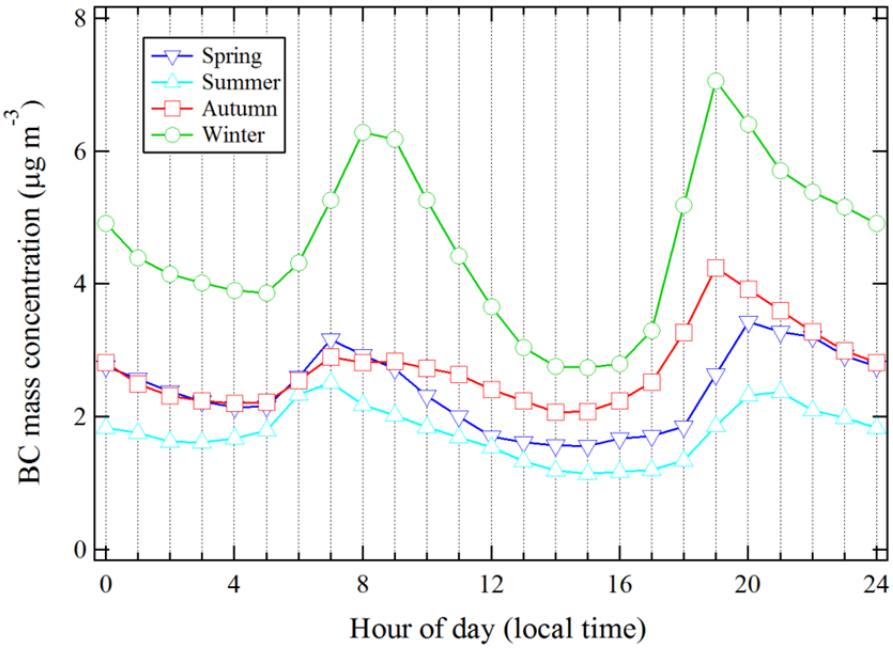

Fig. 5. Diurnal variations of BC mass concentrations in each season.

reached a minimum value (1.6 μg m^{-3} for spring, 1.1 μg m^{-3} for summer, 2.1 μg m^{-3} for autumn, and 2.7 μg m^{-3} for winter) at 14:00–16:00. In the late afternoon, BC started to increase again at a rate of 0.7 μg m^{-3} h^{-1} for spring, 0.4 μg m^{-3} h^{-1} for summer, 1.0 μg m^{-3} h^{-1} for autumn, and 2.2 μg m^{-3} h^{-1} for winter, and it reached a nighttime peak at 19:00–21:00, with an average value of 3.4 μg m^{-3} for spring, 2.4 μg m^{-3} for summer, 4.2 μg m^{-3} for autumn, and 7.1 μg m^{-3} for winter. Thereafter, BC decreased at a rate of 0.2 μg m^{-3} h^{-1} for spring, 0.1 μg m^{-3} h^{-1} for summer, 0.2 μg m^{-3} h^{-1} for autumn, and 0.3 μg m^{-3} h^{-1} for winter until 03:00 when a morning trough was observed.

The BC diurnal variation in Baoji exhibited a typical pattern in urban areas, which has been observed elsewhere (Chen *et al.*, 2014; Feng *et al.*, 2014; Wang *et al.*, 2014; Zhuang *et al.*, 2014). The diurnal cycle of each season was associated with a combination of BC emissions and meteorological conditions. The morning BC peak can be explained by local human activities, particularly rush-hour traffic, and enhanced by the low boundary layer height at the beginning of the day, which leads to the accumulation of pollutants on the surface. With the enhancement in solar radiation as the day proceeds, the height of boundary layer and wind speed increase, leading to a dilution of pollutants and resulting in a trough of BC in the afternoon. The night BC peak was mainly related to the evening rush-hour traffic and other human activities (e.g., heating in winter and cooking). Those impacts were presumably exacerbated by the shallow nocturnal boundary layer caused by radiative cooling. The decreasing trend at night was attributed to the reductions in pollutants from local anthropogenic activities as well as scavenging by dry deposition.

BC Potential Pollution Source Areas

A potential source contribution function (PSCF) model was employed to determine the possible seasonal source areas for BC in Baoji. The PSCF calculation was based on 3-day trajectories using the NOAA Air Resource Lab (ARL) Hybrid Single-Particle Lagrangian Integrated Trajectory (HYSPLIT) model. Gridded meteorological data from the Global Data Assimilation System (GDAS1) was utilized in the HYSPLIT model. The calculated backward trajectories were on the basis of an arrival height of 500 m above ground level. Due to the lack of GDAS1 data in September, only data from October and November were used in PSCF model to represent autumn. In this study, about 2202, 2120, 1412, and 2154 backward trajectories were retrieved in spring, summer, autumn, and winter, respectively.

For the PSCF model, the geographic areas covered by the trajectories were separate into an array of 0.5° latitude × 0.5° longitude. The number of terminated trajectory segment endpoints within each cell was used to calculate PSCF values. For example, an endpoint number falling in the *ij*th cell is defined as $n(i, j)$. The endpoint number for the same cell when the corresponding BC loading is larger than an arbitrarily set criterion value is designated as $m(i, j)$. Finally, the calculation formula of the PSCF value for the *ij*th cell is defined as

$$\mathrm{PSCF}(i,j) = m(i,j)/n(i,j) \quad (1)$$

In the PSCF analysis, some grid cells may contain only one endpoint ($n(i, j) = 1$). If this situation occurs to a pollution event trajectory, then the PSCF value would be 1, but the uncertainty of this result would be large. In this study, a weight function $W(i, j)$ was established to reduce the impact of small $n(i, j)$ value, and the setting principle was when the number of the end points per a particular cell was less than about three times the average values of the end points per cell. Thus, the $W(i, j)$ was set as follows:

$$W(i,j)=\begin{cases}1.00 & 80<n_{ij}\\ 0.70 & 20<n_{ij}\le 80\\ 0.42 & 10<n_{ij}\le 20\\ 0.05 & n_{ij}\le 10\end{cases} \quad (2)$$

Although the PSCF model is a practical tool often used to locate potential source areas (e.g., Zhang *et al.*, 2013b; Dimitriou, 2015; Zhu *et al.*, 2016), a restriction of this method is that the same PSCF values may occur in different grid cells when BC loadings at the receptor site are either substantially larger or only slightly larger than the criterion value, which is often derived as the arithmetic mean (e.g., Wang *et al.*, 2004; Xu and Akhtar, 2010; Zhao *et al.*, 2015). This may lead to difficulties in differentiating heavy pollution sources from moderate ones. To further distinguish, the 75th percentile of each season's data was set as the criterion value, which was 3.0 μg m^{-3} for spring, 2.4 μg m^{-3} for summer, 3.6 μg m^{-3} for autumn, and 5.9 μg m^{-3} for winter. A previous study indicated that a higher criterion value could make better resolution of PSCF source identifications than the mean value (Cheng and Lin, 2001).

The seasonal maps of PSCF results at the arrival height of 500 m are shown in Fig. 6. Distinct potential pollution source regions of BC for Baoji were found in each season. For spring, the largest possible source regions for BC were to the southwest of Baoji. These areas include the south of Shaanxi province (including the cities of Hanzhong, Shangluo, and Ankan), northwest of Hubei province, and north of Chongqing. For summer, the distribution of PSCF values was rather dispersed and the values were lower than 0.6, indicating that the contribution from regional transport was small. For autumn, the possible source regions of BC were to the south of Baoji, mainly in the southwest of Shaanxi province. Considering the high BC loadings in Baoji in autumn, the low PSCF values (< 0.6) indicated a higher possible large BC emission originating from local sources than from regional transport from southern Shaanxi province. For winter, the most likely source regions for BC were located to the southwest of Baoji, mainly in the northeast of the Sichuan Basin, including the cities of Chengdu, Deyang, Suining, Guangyuan, Bazhong, and Dazhou, where BC emissions are considered to be high (Wang *et al.*, 2012).

CONCLUSIONS

The surface characteristics of BC aerosol were measured in Baoji, a midsized urban area in China, from January till December in 2015. The seasonal, monthly, and diurnal variations in BC were investigated, as well as its potential source regions. The annual arithmetic mean of mass concentrations in Baoji was 2.9 ± 1.7 μg m^{-3}, with the highest monthly BC level occurring in January and the lowest in June. The seasonality indicates maximum mean loadings in winter (4.6 ± 2.8 μg m^{-3}), moderate values in spring (2.4 ± 1.6 μg m^{-3}) and autumn (2.7 ± 1.7 μg m^{-3}), and minimums in summer (1.8 ± 0.9 μg m^{-3}). The large BC loadings in winter were attributed to increased domestic heating and stagnant meteorological conditions, whereas the low levels in summer were related to increased precipitation. The mass concentrations exhibited similar bimodal diurnal patterns

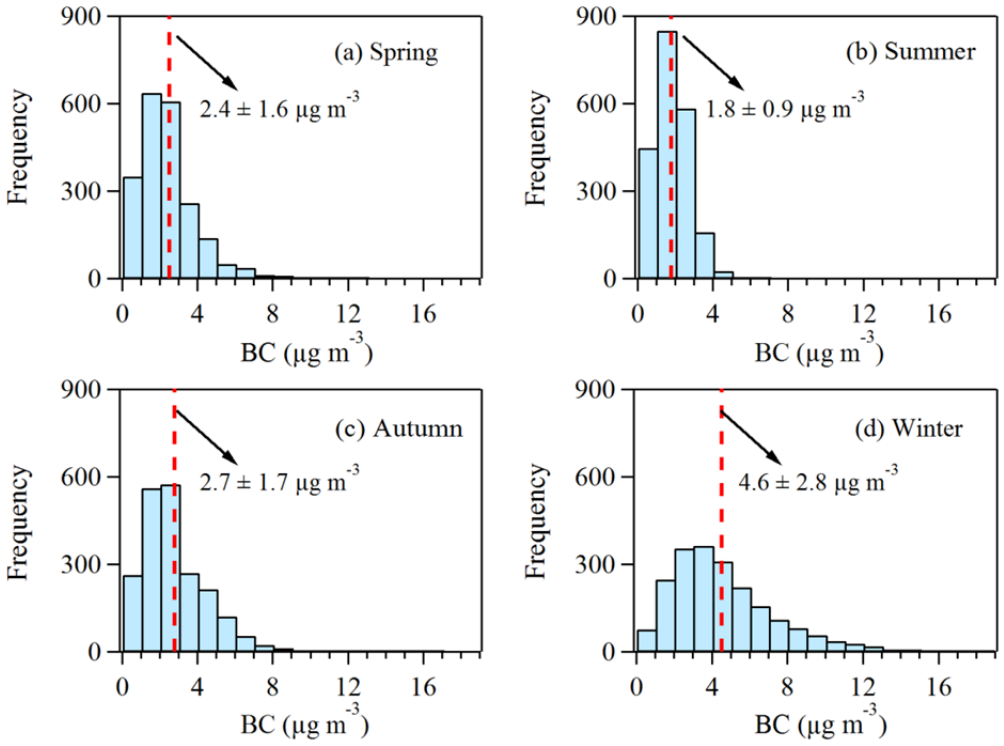

Fig. 6. The maps of likely source areas of BC identified using a potential source contribution function (PSCF) model during each season.

during the four seasons: the peak value occurred during the morning rush hour, decreased to an afternoon trough, then rose again during the evening rush hour, and finally declined at night. The morning and evening peaks are mainly related to the enhanced traffic emissions as well as the low boundary layer and stagnant airflow. The PSCF model indicated that the impacts of regional transport mostly occurred in spring and winter and that local contributions may be more important in summer and autumn. The most likely regional sources of BC in Baoji were southern Shaanxi, northwestern Hubei, and the northern part of Chongqing during spring, whereas the northeastern part of the Sichuan Basin was the most important source region of BC during winter.

ACKNOWLEDGMENTS

This study was supported by the National Natural Science Foundation of China (41503118 and 41325014), the Strategic Priority Research Program of the CAS for Financial Support (XDB05020401), the Science and Technology Coordinating Innovative Engineering Projects of Shaanxi Province (2016KTCL03-17), the Baoji University of Arts and Sciences Key Research Project (14031), and the China Postdoctoral Science Foundation (2015M580890).

REFERENCES

Arnott, W.P., Hamasha, K., Moosmuller, H., Sheridan, P.J. and Ogren, J.A. (2005). Towards aerosol light-absorption measurements with a 7-wavelength aethalometer: evaluation with a photoacoustic instrument and 3-wavelength nephelometer. *Aerosol Sci. Technol.* 39: 17–29.

Bellouin, N., Boucher, O., Haywood, J. and Reddy, M.S. (2005). Global estimate of aerosol direct radiative forcing from satellite measurements. *Nature* 438: 1138–1141.

Bond, T., Zarzycki, C., Flanner, M. and Koch, D. (2011). Quantifying immediate radiative forcing by black carbon and organic matter with the specific forcing pulse. *Atmos. Chem. Phys.* 11: 1505–1525.

Bond, T.C., Doherty, S.J., Fahey, D.W., Forster, P.M., Berntsen, T., DeAngelo, B.J., Flanner, M.G., Ghan, S., Karcher, B., Koch, D., Kinne, S., Kondo, Y., Quinn, P.K., Sarofim, M.C., Schultz, M.G., Schulz, M., Venkataraman, C., Zhang, H., Zhang, S., Bellouin, N., Guttikunda, S.K., Hopke, P.K., Jacobson, M.Z., Kaiser, J.W., Klimont, Z., Lohmann, U., Schwarz, J.P., Shindell, D., Storelvmo, T., Warren, S.G. and Zender, C.S. (2013). Bounding the role of black carbon in the climate system: A scientific assessment. *J. Geophys. Res. Atmos.* 118: 5380–5552.

Cao, J.J., Zhu, C.S., Chow, J.C., Watson, J.G., Han, Y.M., Wang, G.H., Shen, Z.X. and An, Z.S. (2009). Black carbon relationships with emissions and meteorology in Xi'an, China. *Atmos. Res.* 94: 194–202.

Chen, X., Zhang, Z., Engling, G., Zhang, R., Tao, J., Lin, M., Sang, X., Chan, C., Li, S. and Li, Y. (2014). Characterization of fine particulate black carbon in Guangzhou, a megacity of south China. *Atmos. Pollut. Res.* 5: 361–370.

Chen, Y., Schleicher, N., Fricker, M., Cen, K., Liu, X.L., Kaminski, U., Yu, Y., Wu, X.F. and Norra, S. (2016). Long-term variation of black carbon and $PM_{2.5}$ in Beijing, China with respect to meteorological conditions and governmental measures. *Environ. Pollut.* 212: 269–278.

Cheng, M.D. and Lin, C.J. (2001). Receptor modeling for smoke of 1998 biomass burning in central America. *J. Geophys. Res.* 106: 22871–22886.

Cheng, T., Han, Z., Zhang, R., Du, H., Jia, X., Wang, J. and Yao, J. (2010). Black carbon in a continental semi-arid area of Northeast China and its possible sources of fire emission. *J. Geophys. Res.* 115: D23204.

Corrigan, C.E., Ramanathan, V. and Schauer, J.J. (2006). Impact of monsoon transitions on the physical and optical properties of aerosols. *J. Geophys. Res.* 111: D18208.

Dimitriou, K. (2015). The dependence of PM size distribution from meteorology and local-regional contributions, in Valencia (Spain) – A CWT model approach. *Aerosol Air Qual. Res.* 15: 1979–1989.

Feng, J., Zhong, M., Xu, B., Du, Y., Wu, M., Wang, H. and Chen, C. (2014). Concentrations, seasonal and diurnal variations of black carbon in $PM_{2.5}$ in Shanghai, China. *Atmos. Res.* 147–148: 1–9.

Gong, W., Zhang, T., Zhu, Z., Ma, Y., Ma, X. and Wang, W. (2015). Characteristics of $PM_{1.0}$, $PM_{2.5}$, and PM_{10}, and their relation to black carbon in Wuhan, Central China. *Atmosphere* 6: 1377–1387.

Gordon, H., Sengupta, K., Rap, A., Duplissy, J., Frege, C., Williamson, C., Heinritzi, M., Simon, M., Yan, C., Almeida, J., Trostl, J., Nieminen, T., Ortega, I.K., Wagner, R., Dunne, E.M., Adamov, A., Amorim, A., Bernhammer, A.K., Bianchi, F., Breitenlechner, M., Brilke, S., Chen, X., Craven, J.S., Dias, A., Ehrhart, S., Fischer, L., Flagan, R.C., Franchin, A., Fuchs, C., Guida, R., Hakala, J., Hoyle, C.R., Jokinen, T., Junninen, H., Kangasluoma, J., Kim, J., Kirkby, J., Krapf, M., Kuerten, A., Laaksonen, A., Lehtipalo, K., Makhmutov, V., Mathot, S., Molteni, U., Monks, S.A., Onnela, A., Perakyla, O., Piel, F., Petaja, T., Praplan, A.P., Pringle, K.J., Richards, N.A.D., Rissanen, M.P., Rondo, L., Sarnela, N., Schobesberger, S., Scott, C.E., Seinfeldo, J.H., Sharma, S., Sipila, M., Steiner, G., Stozhkov, Y., Stratmann, F., Tome, A., Virtanen, A., Vogel, A.L., Wagner, A.C., Wagner, P.E., Weingartner, E., Wimmer, D., Winkler, P.M., Ye, P., Zhang, X., Hansel, A., Dommen, J., Donahue, N.M., Worsnop, D.R., Baltensperger, U., Kulmala, M., Curtius, J. and Carslaw, K.S. (2016). Reduced anthropogenic aerosol radiative forcing caused by biogenic new particle formation. *Proc. Natl. Acad. Sci. U.S.A.* 113: 12053–12058.

Heal, M.R., Kumar, P. and Harrison, R.M. (2012). Particles, air quality, policy and health. *Chem. Soc. Rev.* 41: 6606–6630.

Jacobson, M.Z. (2001). Strong radiative heating due to the mixing state of black carbon in atmospheric aerosols. *Nature* 409: 695–697.

Janssen, N.A., Hoek, G., Simic-Lawson, M., Fischer, P., Van Bree, L., Ten Brink, H., Keuken, M., Atkinson, R.W., Anderson, H.R. and Brunekreef, B. (2011). Black

carbon as an additional indicator of the adverse health effects of airborne particles compared with PM_{10} and $PM_{2.5}$. *Environ. Health Perspect.* 119: 1691–1699.

Kahn, R.A. (2012). Reducing the uncertainties in direct aerosol radiative forcing. *Surv. Geophys.* 33: 701–721.

Kim, D., Wang, C., Ekman, A.M., Barth, M.C. and Rasch, P.J. (2008). Distribution and direct radiative forcing of carbonaceous and sulfate aerosols in an interactive size-resolving aerosol-climate model. *J. Geophys. Res.* 113: D16309.

Lee, L.A., Reddington, C.L. and Carslaw, K.S. (2016). On the relationship between aerosol model uncertainty and radiative forcing uncertainty. *Proc. Natl. Acad. Sci. U.S.A.* 113: 5820–5827.

Liu, J., Fan, S., Horowitz, L.W. and Levy, H. (2011). Evaluation of factors controlling long-range transport of black carbon to the arctic. *J. Geophys. Res.* 116: D04307.

Lyamani, H., Olmo, F.J., Foyo, I. and Alados-Arboledas, L. (2011). Black carbon aerosols over an urban area in south-eastern Spain: Changes detected after the 2008 economic crisis. *Atmos. Environ.* 45: 6423–6432.

Moorthy, K.K., Babu, S.S., Badarinath, K.V.S., Sunilkumar, S.V., Kiranchand, T.R. and Ahmed, Y.N. (2007). Latitudinal distribution of aerosol black carbon and its mass fraction to composite aerosols over peninsular India during winter season. *Geophys. Res. Lett.* 34: L08802.

Nair, V.S., Moorthy, K.K., Alappattu, D.P., Kunhikrishnan, P.K., George, S., Nair, P.R., Babu, S.S., Abish, B., Satheesh, S.K., Tripathi, S.N., Niranjan, K., Madhavan, B.L., Srikant, V., Dutt, C.B.S., Badarinath, K.V.S. and Reddy, R.R. (2007). Wintertime aerosol characteristics over the Indo-Gangetic Plain (IGP): Impacts of local boundary layer processes and long-range transport. *J. Geophys. Res* 112: D13205.

Putero, D., Cristofanelli, P., Marinoni, A., Adhikary, B., Duchi, R., Shrestha, S.D., Verza, G.P., Landi, T.C., Calzolari, F., Busetto, M., Agrillo, G., Biancofiore, F., Di Carlo, P., Panday, A.K., Rupakheti, M. and Bonasoni, P. (2015). Seasonal variation of ozone and black carbon observed at Paknajol, an urban site in the Kathmandu Valley, Nepal. *Atmos. Chem. Phys.* 15: 13957–13971.

Ran, L., Deng, Z.Z., Wang, P.C. and Xia, X.A. (2016). Black carbon and wavelength-dependent aerosol absorption in the North China Plain based on two-year aethalometer measurements. *Atmos. Environ.* 142: 132–144.

Rattigan, O.V., Civerolo, K., Doraiswamy, P., Felton, H.D., and Hopke, P.K. (2013). Long term black carbon measurements at two urban locations in New York. *Aerosol Air Qual. Res.* 13: 1181–1196.

Reddy, B.S.K., Kumar, K.R., Balakrishnaiah, G., Gopal, K.R., Reddy, R., Reddy, L., Ahammed, Y.N., Narasimhulu, K., Moorthy, K.K. and Babu, S.S. (2012). Potential source regions contributing to seasonal variations of black carbon aerosols over anantapur in southeast India. *Aerosol Air Qual. Res.* 12: 344–358.

Retama, A., Baumgardner, D., Raga, G.B., McMeeking, G.R. and Walker, J.W. (2015). Seasonal and diurnal trends in black carbon properties and co-pollutants in Mexico city. *Atmos. Chem. Phys.* 15: 9693–9709.

Saha, A. and Despiau, S. (2009). Seasonal and diurnal variations of black carbon aerosols over a mediterranean coastal zone. *Atmos. Res.* 92: 27–41.

Shen, L., Li, L., Lü, S., Zhang, X., Liu, J., An, J., Zhang, G., Wu, B. and Wang, F. (2015). Characteristics of black carbon aerosol in Jiaxing, China during autumn 2013. *Particuology* 20: 10–15.

Targino, A.C. and Krecl, P. (2016). Local and regional contributions to black carbon aerosols in a mid-sized city in southern Brazil. *Aerosol Air Qual. Res.* 16: 125–137.

Tiwari, S., Srivastava, A.K., Bisht, D.S., Parmita, P., Srivastava, M.K. and Attri, S.D. (2013). Diurnal and seasonal variations of black carbon and $PM_{2.5}$ over New Delhi, India: Influence of meteorology. *Atmos. Res.* 125–126: 50–62.

Virkkula, A., Makela, T., Hillamo, R., Yli-Tuomi, T., Hirsikko, A., Hameri, K. and Koponen, I.K. (2007). A simple procedure for correcting loading effects of aethalometer data. *J. Air Waste Manage. Assoc.* 57: 1214–1222.

Wang, Q., Cao, J., Tao, J., Li, N., Su, X., Chen, L.W.A., Wang, P., Shen, Z., Liu, S. and Dai, W. (2013). Long-term trends in visibility and at Chengdu, China. *PLoS One* 8: e68894.

Wang, Q., Huang, R..J., Cao, J., Han, Y., Wang, G., Li, G., Wang, Y., Dai, W., Zhang, R. and Zhou, Y. (2014). Mixing state of black carbon aerosol in a heavily polluted urban area of China: Implications for light absorption enhancement. *Aerosol Sci. Technol.* 48: 689–697.

Wang, Q., Huang, R.J., Cao, J., Tie, X., Shen, Z., Zhao, S., Han, Y., Li, G., Li, Z., Ni, H., Zhou, Y., Wang, M., Chen, Y. and Su, X. (2016a). Contribution of regional transport to the black carbon aerosol during winter haze period in Beijing. *Atmos. Environ.* 132: 11–18.

Wang, Q., Huang, R..J., Zhao, Z., Zhang, N., Wang, Y., Ni, H., Tie, X., Han, Y., Zhuang, M., Wang, M., Zhang, J., Zhang, X., Dusek, U. and Cao, J. (2016b). Size distribution and mixing state of refractory black carbon aerosol from a coastal city in south China. *Atmos. Res.* 181: 163–171.

Wang, Q.Y., Huang, R.J., Cao, J.J., Tie, X.X., Ni, H.Y., Zhou, Y.Q., Han, Y.M., Hu, T.F., Zhu, C.S., Feng, T., Li, N. and Li, J.D. (2015). Black carbon aerosol in winter northeastern Qinghai-Tibetan Plateau, China: the source, mixing state and optical property. *Atmos. Chem. Phys.* 15: 13059–13069.

Wang, R., Tao, S., Wang, W., Liu, J., Shen, H., Shen, G., Wang, B., Liu, X., Li, W., Huang, Y., Zhang, Y., Lu, Y., Chen, H., Chen, Y., Wang, C., Zhu, D., Wang, X., Li, B., Liu, W. and Ma, J. (2012). Black carbon emissions in China from 1949 to 2050. *Environ. Sci. Technol.* 46: 7595–7603.

Wang, Y.Q., Zhang, X.Y., Arimoto, R., Cao, J.J. and Shen, Z.X. (2004). The transport pathways and sources of PM_{10} pollution in Beijing during spring 2001, 2002 and 2003. *Geophys. Res. Lett.* 31: L14110.

Wu, D. (2004). *Demographics of the county and city in China*. Department of the Ministry of Public Security, China, Qunzhong Press, Beijing, pp. 91–106.

Wu, D., Wu, C., Liao, B., Chen, H., Wu, M., Li, F., Tan, H.,

Deng, T., Li, H., Jiang, D. and Yu, J.Z. (2013). Black carbon over the South China Sea and in various continental locations in South China. *Atmos. Chem. Phys.* 13: 12257–12270.

Wu, Y., Zhang, R., Pu, Y., Zhang, L., Ho, K.F. and Fu, C. (2012). Aerosol optical properties observed at a semi-arid rural site in northeastern China. *Aerosol Air Qual. Res.* 12: 503–514.

Xiao, S., Wang, Q., Cao, J., Huang, R.J., Chen, W., Han, Y., Xu, H., Liu, S., Zhou, Y. and Wang, P. (2014). Long-term trends in visibility and impacts of aerosol composition on visibility impairment in Baoji, China. *Atmos. Res.* 149: 88–95.

Xu, X. and Akhtar, U.S. (2010). Identification of potential regional sources of atmospheric total gaseous mercury in Windsor, Ontario, Canada using hybrid receptor modeling. *Atmos. Chemis. Phys.* 10: 7073–7083.

Zhang, N., Qin, Y. and Xie, S. (2013a). Spatial distribution of black carbon emissions in China. *Chin. Sci. Bull.* 58: 3830–3839.

Zhang, R., Jing, J., Tao, J., Hsu, S.C., Wang, G., Cao, J., Lee, C.S.L., Zhu, L., Chen, Z., Zhao, Y. and Shen, Z. (2013b). Chemical characterization and source apportionment of $PM_{2.5}$ in Beijing: Seasonal perspective. *Atmos. Chem. Phys.* 13: 7053–7074.

Zhang, X., Rao, R., Huang, Y., Mao, M., Berg, M.J. and Sun, W. (2015). Black carbon aerosols in urban central China. *J. Quant. Spectrosc. Radiat. Transfer* 150: 3–11.

Zhang, X.Y., Wang, Y.Q., Niu, T., Zhang, X.C., Gong, S.L., Zhang, Y.M. and Sun, J.Y. (2012). Atmospheric aerosol compositions in China: spatial/temporal variability, chemical signature, regional haze distribution and comparisons with global aerosols. *Atmos. Chem. Phys.* 12: 779–799.

Zhao, M., Huang, Z., Qiao, T., Zhang, Y., Xiu, G. and Yu, J. (2015). Chemical characterization, the transport pathways and potential sources of $PM_{2.5}$ in Shanghai: Seasonal variations. *Atmos. Res.* 158: 66–78.

Zhao, P., Dong, F., Yang, Y., He, D., Zhao, X., Zhang, W., Yao, Q. and Liu, H. (2013). Characteristics of carbonaceous aerosol in the region of Beijing, Tianjin, and Hebei, China. *Atmos. Environ.* 71: 389–398.

Zhou, J., Zhang, R., Cao, J., Chow, J.C. and Watson, J.G. (2012). Carbonaceous and ionic components of atmospheric fine particles in Beijing and their impact on atmospheric visibility. *Aerosol Air Qual. Res.* 12: 492–502.

Zhu, C.S., Cao, J.J., Xu, B.Q., Huang, R.J., Wang, P., Ho, K.F., Shen, Z.X., Liu, S.X., Han, Y.M., Tie, X.X., Zhao, Z.Z. and Chen, L.W.A. (2016). Black carbon aerosols at Mt. Muztagh Ata, a high-altitude location in the western Tibetan Plateau. *Aerosol Air Qual. Res.* 16: 752–763.

Zhuang, B.L., Wang, T.J., Liu, J., Li, S., Xie, M., Yang, X.Q., Fu, C.B., Sun, J.N., Yin, C.Q., Liao, J.B., Zhu, J.L. and Zhang, Y. (2014). Continuous measurement of black carbon aerosol in urban Nanjing of Yangtze River Delta, China. *Atmos. Environ.* 89: 415–424.

Received for review, February 22, 2017
Revised, October 10, 2017
Accepted, October 24, 2017